

RINTC-E PROJECT: TOWARDS THE ASSESSMENT OF THE SEISMIC RISK OF EXISTING BUILDINGS IN ITALY

Iunio Iervolino,¹ Andrea Spillatura,² Paolo Bazzurro³

¹ Dipartimento di Strutture per l'Ingegneria e l'Architettura
Università degli Studi di Napoli Federico II Naples, Italy
e-mail: iunio.iervolino@unina.it

² European Centre for Training and Research in
Earthquake Engineering (EUCENTRE) Pavia, Italy
andrea.spillatura@gmail.com

³ University School for Advanced Studies of Pavia
(IUSS Pavia) Pavia, Italy
paolo.bazzurro@iusspavia.it

Abstract

The 2019-2021 RINTC project is the extension of the 2015-2017 RINTC project that assessed, explicitly, the seismic risk of code-conforming Italian structures (i.e., designed according to the seismic code currently enforced). The aim of the new RINTC project is to extend the methodological framework developed in RINTC to the existing structures (designed and built before 2008), which constitute the vast majority of Italian building stock. In 2018 some analyses, preliminary with respect to the 2019-2021 project, were carried out; i.e., the 2018 RINTC-e project. In particular, five structural typologies were considered: masonry, reinforced concrete, pre-cast reinforced concrete, steel, and seismically isolated buildings. In the framework of the 2018 project, several archetype structures for each typology have been designed and/or retrofitted according to standard practices consistent with outdated codes, enforced since the eighties, for five sites across Italy spanning a wide range of seismic hazard levels (evaluated according to current standards). The seismic vulnerability of the designed structures was assessed by subjecting three-dimensional nonlinear computer models to multi-stripe non-linear dynamic analysis. Integration of the probabilistic hazard and probabilistic vulnerability (i.e., fragility) yields the annual failure rate for each of the designed and modeled structure. In the paper, the 2019-2021 RINTC project is introduced and the preliminary failure rates of the existing structures are presented.

Keywords: Reliability, Structures, Earthquake Engineering, Failure, Damage.

1 INTRODUCTION

The 2015-2017 RINTC (*Rischio Implicito delle strutture progettate secondo le NTC*) project was a large research effort aimed at assessing the seismic structural reliability, expressed in terms of annual failure rate, of code-conforming structures in Italy [1][3]. For the purposes of the project three sites exposed to comparatively low- mid- and high-seismic hazard were considered; i.e., Milan (MI), Naples (NA) and L'Aquila (AQ). At these sites, residential/industrial buildings belonging to five structural typologies were designed according to the recent Italian seismic code; i.e., un-reinforced masonry (URM), reinforced concrete (RC), pre-cast reinforced concrete (PRC), steel (S), and base-isolated (BI) structures. All typologies were designed at all sites with reference to two limit states considered by the code; *damage control* and *life-safety*. Three-dimensional non-linear models were developed for the buildings, with the aim of running dynamic analysis for performance assessment with respect to two ad-hoc defined failure conditions: *usability-preventing damage* (UPD) and *global collapse* (GC). Earthquake records for the non-linear dynamic analysis were selected according to the *conditional-spectrum* (CS) [4] approach. The results mainly indicate that the seismic structural reliability changes by orders of magnitude as the seismic hazard changes from site-to-site, despite homogeneity of the exceedance return period of the design ground motion and of the other design and modelling choices. The contribution of uncertainty in modelling assumptions and soil-structure interaction was also quantified and found of relatively minor importance.

Herein the 2019-2021 RINTC project is introduced. It targets the seismic structural reliability of *low-* and *pre-code* structures in Italy. This is because these structures constitute the vast majority of the Italian building stock. To compare the reliability results to those already obtained for the code-conforming structures, the modelling and analysis framework is retained from the previous project. Three code levels, previous to the contemporary era, are broadly identified for the existing structures in Italy: (1) the 80-90s; (2) the 70s; (3) the pre-70s era. While (1) and (2) represent ages of evolution of the codes toward modern earthquake-resistant design, (3) is when most of the buildings in Italy were designed basically for gravity loads.

In this short paper, the workplan, in terms of analyzed structures, is presented together with the preliminary results from the preparatory activity developed in 2018. In particular the 2018 RINTC-e project is discussed. To this aim, the following is organized such that the case studies of the 2019-2021 RINTC project are illustrated. Subsequently, the structures analyzed in 2018, mostly referring to design or seismic upgrade of structures according to the codes enforced in the 80-90s (some also from the 70s) in Italy, are described along with the representation of the ground motion for reliability assessment via non-linear dynamic analysis. Then, the failure criteria considered, analogous to the 2015-2017 RINTC project are recalled. Finally, the, very preliminary, results in terms of failure rates are discussed. Final remarks close the paper.

2 RINTC-E SITES, STRUCTURES AND BUILDING CODES

The RINTC 2019-2021 project deals with existing buildings built, essentially, in the XX century, in which the design in Italy evolved from only gravity-load-design all-over the country to earthquake-resistant design in most of the country [5]. All the considered codes precede the contemporary era in which seismic actions are based on probabilistic seismic hazard analysis and the principle of seismic design (e.g., *capacity design*) are fully acknowledged by the code.

Table 1 provides a matrix where the buildings considered in the 2019-2021 project are associated to the design/construction age and the sites where they are supposed¹ to be located. It is to note that two sites, Rome (RM) and Catania (CT), have been specifically-considered for the purposes of the RINTC-e project. In particular, Catania has been considered as a site with relatively high seismic hazard according to the current code, yet characterized by gravity-load design only since a few decades ago. The addition of Rome downtown allowed to consider large URM buildings typical of historical downtowns in Italy, similar to Naples, yet exposed to different seismic hazard. Figure 1 (left), shows the considered sites overlaid on the map of the *peak ground acceleration* (PGA) with 475 years exceedance return period on rock, which is adopted by the current code as a basis to determine the current design actions [6],[7]. Figure 1 (right) shows the PGA on rock hazard curves for the five sites, ad-hoc computed, yet consistent with the probabilistic seismic hazard study at the basis of the current code [8]. The relative seismic design hazard levels can be observed from the figure. MI is the less hazardous and AQ is the most hazardous.

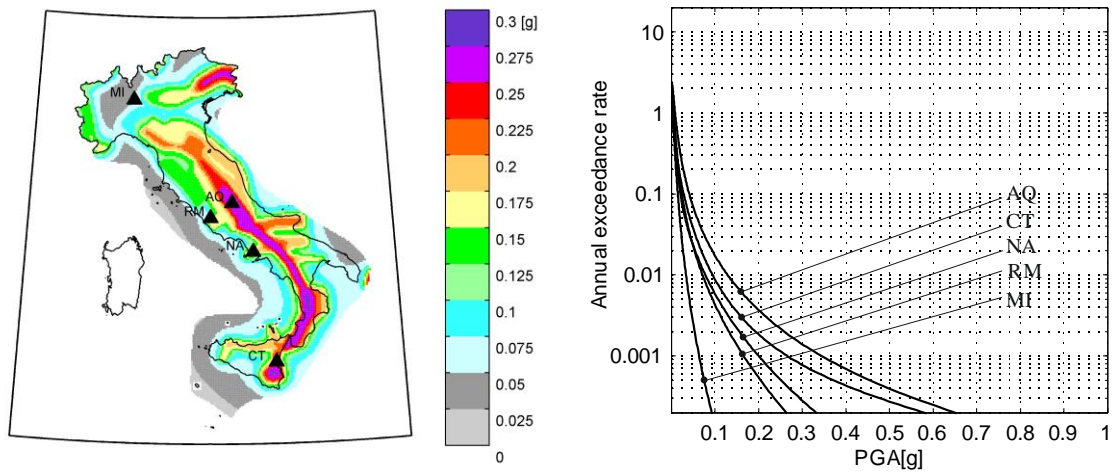


Figure 1: Left – considered sites on the map of peak ground acceleration (PGA) with 475 years exceedance return period on rock, adopted by the current code; right – PGA hazard curves on rock for the five sites.

Table 1: Building/sites matrix for the existing buildings to be studied in the 2019-2021 RINTC project and those analyzed in the 2018 RINTC-e project (in bold).²

	<i>Milan (MI)</i>	<i>Rome (RM)</i>	<i>Naples (NA)</i>	<i>Catania (CT)</i>	<i>L'Aquila (AQ)</i>
<i>RC</i>	G(50s-60s), G(70s) , G(80s-90s),		G(50s-60s), G(70s) , G(80s-90s),	G(50s-60s), G(70s) , G(80s-90s)	S(50s-60s), S(70s), S(80s-90s)
<i>URM</i>	G(<20s), G(20s-40s)	G(90s), SU(80s-90s), SU(08-18), SU(NTC)rs1 , SU(NTC)rs2	G(<20s), SU(NTC)str1 , SU(NTC)str2 , SU(POR)str1 , SU(POR)str2	G(<20s), G(50s-60s)	G(<20s), SU(80s-90s), SU(2008-2018)

¹ URM buildings in Rome are actual buildings located in the city's downtown.

² G = gravity-load-design; S = earthquake-resistant design; SU = seismically upgraded (see [9] for RC and [10] for PRC); NTC = current Italian code [6], POR = analysis method (see [11]), str-1,2= structure type, rs-1,2 = rehabilitation strategy (see [11]); HP = portal with Hinges, FP= fully constrained portal, SP = sandwich panels, TS = trapezoidal sheeting (see [12]); BI-G,S= RC structures isolated with high-damping rubber bearing and/or sliders (HDRB) or double-curvature friction pendulums (DCFP) (see [13]). Numbers in the parentheses represent reference years for code provisions used for design.

<i>PRC</i>	G(70s) , G(60s-80s), G(80s-90s)		G(70s) , G(60s-80s), S(80s-90s)	G(70s)	S(60s-80s), S(80s-90s), S(80s-90s)
<i>S</i>	FP-SP(80s-90s), HP-TS(80s-90s), HP-SP(80s-90s)		FP-SP(80s-90s), HP-TS(80s-90s), HP-SP(80s-90s)		FP-SP(80s-90s), HP-BF(80s-90s) , HP-TS(80s-90s) , HP-SP(80s-90s)
<i>BI</i>			BI-G(50s-60s), BI-G(70s) , G(80s-90s)		BI-S(50s-60s), BI-S(70s), BI-S(80s-90s)

The failure rates of buildings in bold in Table 1 are preliminarily addressed in this paper. The considered codes, although modern, are not at the contemporary level of seismic design, at least in terms of definition of design action and resistant mechanism rules such as capacity design. In most of cases, buildings were designed according to these codes; however, in the case of unreinforced masonry, older buildings were upgraded according to the considered code or, in some cases according to the current code, indicated as NTC [6]. In the following, few details for each typology are given; however, the interested reader should refer to the specific papers cited for a more comprehensive discussion about design, modelling and analysis.

2.1 URM buildings

For what concerns URM buildings, the 2018 RINTC-e plan was to retrofit older buildings. Retrofit interventions on URM buildings were designed according to the code, issued 1981, for repair and strengthening of buildings damaged by earthquakes [14], and the associated guidelines [15]. These documents incorporate the so-called POR method, originally proposed by Tomazevic [16], for the seismic analysis of retrofitted URM buildings. The relevance of this code is that it was published after the magnitude (M) 6.5 1976 (Friuli, northern Italy), M5.8 1979 (Norcia, southern Italy) and M6.9 1980 (Irpina, southern Italy) earthquakes, and then extensively used in the reconstruction phases. Interventions were also alternatively designed according to the current code (NTC). Eventually, retrofit interventions were assessed according to the code update published in 2018 [7]. As an example, Figure 2 reports the upgraded buildings in Naples, about which further details can be found in [11].

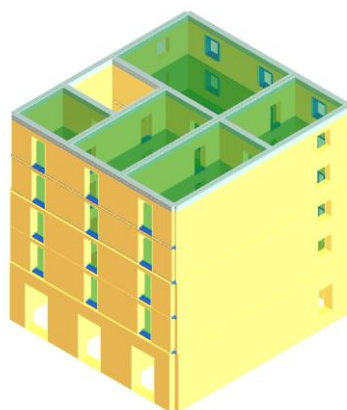


Figure 2: the URM building analyzed in Naples.

2.2 RC buildings

In 2018, case-study structures representative of the existing residential RC building stock in Italy were defined through a simulated design process. These structures were three-storey

buildings, designed for gravity loads only during the 70s (gravity-load-design, G) or for seismic loads during 80s-90s (seismic-load-design, S). G-buildings were designed according to [17]. S-buildings were designed according to [18], as technical code, and to [19], for seismic load provisions. S-buildings were assumed to be located in L'Aquila (*second seismic category* at the time of design; i.e., mid seismic loads in a set of three), and thereby they were designed with a base shear equal to 0.07 times the building weight, adopting a linear static analysis method. Both for G- and S-buildings, the allowable stress design method was used. In all cases modelling considered infilled structures. Details are given in [9], while Figure 3 provides an example of a three-storey RC building.

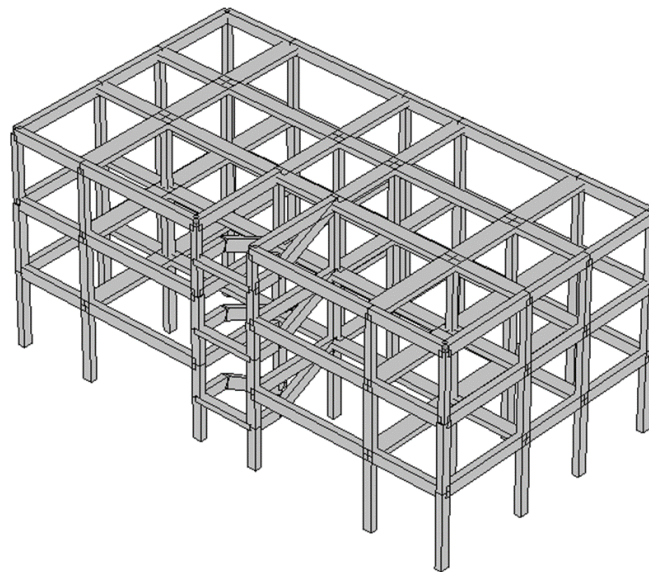


Figure 3: Three-dimensional view of a three-storey S building.

2.3 PRC buildings

Six different single-story PRC buildings were designed according to [17] and [20], enforced in Italy in the 70s, for three different sites (MI, NA, CT) and for two different heights of the columns (6 and 9 m).. The considered codes do not take into account seismic loads and the design follows a deterministic approach according to the allowable stress design. Roof elements and beams are designed only for vertical loads (dead and live loads), whereas the design of columns takes into account the wind load and temperature variations, which are the only horizontal forces acting on the buildings in the design phase. In fact, single-story PRC buildings are also designed according to the seismic codes enforced in Italy in 80s and 90s. Details are given in [10], while Figure 4 provides the front and plan views of the typical PRC buildings designed and modelled in the project.

2.4 S buildings

The building structures were obtained by simulating a design carried out according to the code and standards for steel buildings enforced in the years 1980s-1990s [19],[21][22]. In more detail, [21] contained information regarding variable load values (i.e., wind and snow loads and variable gravity loads). Instead, [19] contained information about the site seismic

classification and the consequent calculation of the equivalent static forces, for both horizontal and vertical components. In addition, [22] was a well know guideline for specific design of steel structures, in terms of resistance, stability and deformability checks. Steel structures design contemplated only hinged-portal (HP) in 2018, while corresponding fully-constrained portals (FP) will be examined in 2019-2021. Concerning the cladding, both sandwich panels (SP) and trapezoidal sheeting (TS), were considered. Details are given in [12], while Figure 3 provides a three-dimensional view of the typical steel building designed and modelled in the project.

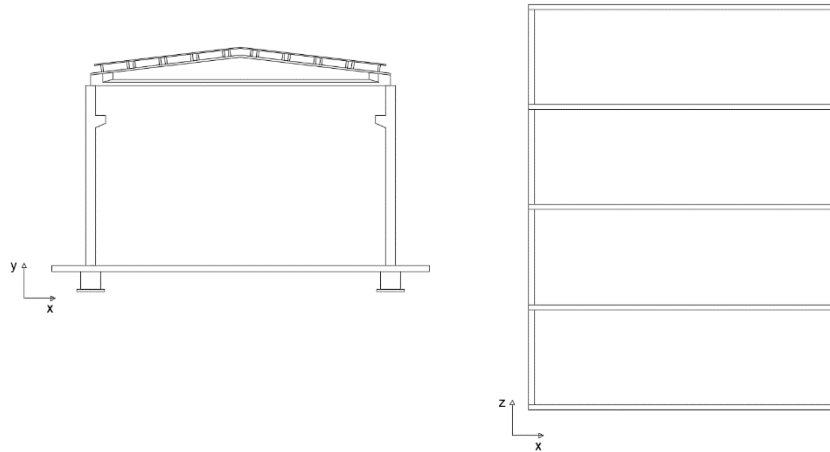


Figure 4: Front (left) and plan (right) views of the typical PRC buildings designed and modelled in the project.

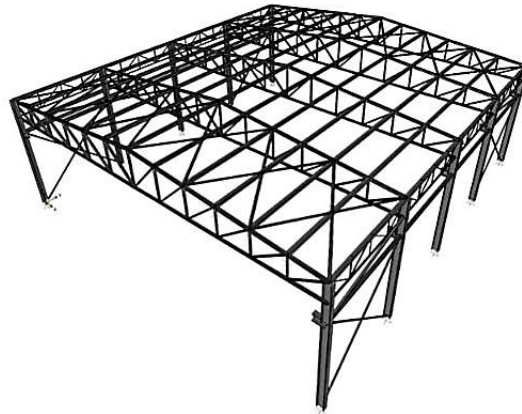


Figure 5: Three-dimensional view of the typical steel building designed herein.

2.5 BI buildings

For the case of BI, the objective was not to design the isolation system according to old codes, yet to protect the existing buildings according to the current code [6],[7]. In particular, for the existing fixed-base RC building (see Table 2), the base shear associated with the onset of plastic deformations was first identified by pushover analysis, assuming a uniform distribution of lateral forces. After that, the lowest value of the fundamental period of the base isolated building was derived entering the design spectrum with the spectral acceleration associated to the occurrence of the first plastic hinge. Next, the maximum displacement of the isolation system was evaluated using the displacement (code) spectrum at the *collapse* limit-state.

Based on the target period and required displacement capacity, suitable devices were selected from the manufacturers' catalogues. The verification of the base-isolated building was carried out through response spectrum analysis of a three-dimensional model of the structure, considering the performance requirements and compliance criteria specified in the current code. See [13] for details.

3 FAILURE CRITERIA

The failure rates were computed with respect to two performance levels, global collapse and usability-preventing damage. In general, the GC criterion is based on the deformation capacity corresponding to a certain level of strength deterioration, measured on the nonlinear static capacity curves of the structural models (Figure 6, left).³ For all the structural models in any dynamic analysis, the occurrence of GC was checked using the maximum demand-over-capacity ratio in the two directions.

The criteria for UPD are based on a multi-criteria approach (Figure 6, right) that considers the onset of any of the following three conditions: (a) light damage in 50% of the main non-structural elements (e.g., infills); (b) at least one of the non-structural elements reached a severe damage level leading to significant interruption of use; (c) attainment of 95% of the maximum base-shear of the structure. Although these are the general criteria, several existing buildings belonging to the case studies analyzed required ad-hoc adjustments and further considerations about failure. The details on these issues are given in the companion articles for these specific typologies.

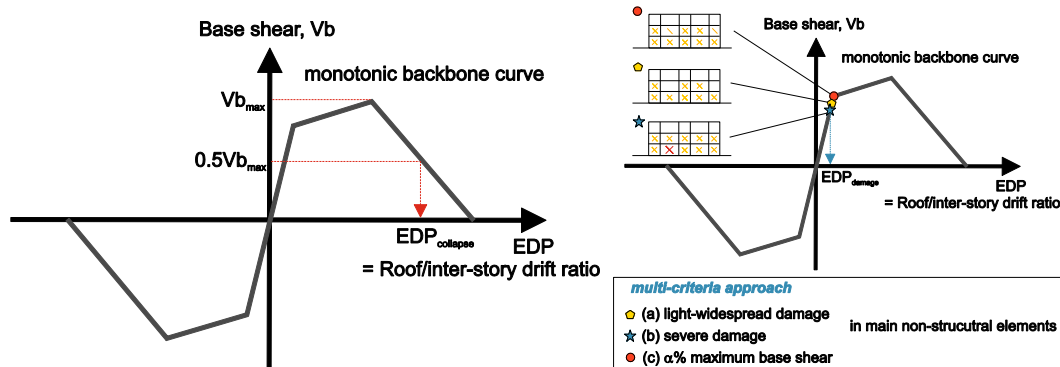


Figure 6: left – general definition for the GC failure criterion; right – general definition of the UPD failure criterion. (Figure adapted from [3])

4 SEISMIC HAZARD AND RECORDS FOR DYNAMIC ANALYSIS

To compute the failure rates, hazard curves are required (see section 8). The ground motion intensity measures (IMs) considered are pseudo-spectral acceleration Sa at periods (T) close to the first-mode periods of the developed structural models. Table 2 reports the ground motion intensity measures the pseudo-spectral accelerations considered at the sites. The table acknowledges that the soil class for the analysis (and for the design, where applicable), was C according to the site classification of Eurocode 8 [23].

The hazard curves, expressed in terms of annual exceedance rate, $\lambda_{Sa(T)}(x)$, versus ground motion intensity, needed for the calculations, were computed as described in [3], that

³ The GC condition for BI buildings was assumed to occur either if the superstructure fails or if the base isolation system fails.

is using the seismic zone source model of [8], with the magnitude distribution and rates described in [24], and the ground motion prediction equation of [25] (or that of [26] for the longer spectral periods not covered by [25]). Hazard calculations have been carried out via the OPENQUAKE platform [27].

Table 2: periods at which pseudo-spectral acceleration hazard has been computed at each site for record selection and failure rate computation.

Site	Soil C
<i>MI</i>	$T = \{0.5s, 1.0s, 2.0s\}$
<i>NA</i>	$T = \{0.25s, 0.5s, 1.0s, 2.0s, 3.0s\}$
<i>RM</i>	$T = \{0.15s, 0.5s\}$
<i>CT</i>	$T = \{0.5s, 1.0s, 2.0s\}$
<i>AQ</i>	$T = \{0.5s, 1.0s, 2.0s, 3.0s\}$

Hazard curves were discretized in ten IM values corresponding to the following return periods (T_R) in years: $T_R = \{10, 50, 100, 250, 500, 1000, 2500, 5000, 10000, 100000\}$. No IM-values with exceedance return period longer than $T_R = 100000yr$ were calculated, to avoid large extrapolations.

To select the ground motion records to be used as input for dynamic analysis, the CS approach has been considered, in analogy to what done in [3]. It accounts for seismic hazard disaggregation, to fit the scopes of non-linear dynamic multi-stripe analysis (MSA), which was used to assess seismic structural vulnerability.

The record selection procedure was that available at http://web.stanford.edu/~bakerjw/research/conditional_spectrum.html. The selected records were extracted mainly from the Italian accelerometric archive (<http://itaca.mi.ingv.it/>; [28]) and only if no records with similar spectra were available there, suitable records in the NGAwest2 (<http://peer.berkeley.edu/ngawest2/>) database [29] were selected instead.

The record selection delivered two-hundreds pairs of records for each IM; twenty records for each one of the ten stripes. Hence, two-hundred records have been employed in the analysis of each individual structural model. To reduce the computational demand from non-linear dynamic analysis, the selected records have been post processed to remove the parts of the signal outside $\{t_{0.05\%}, t_{99.95\%}\}$ range, where $D_{99.90\%} = t_{99.95\%} - t_{0.05\%}$ is the 99.90% significant duration of the record [30], yet keeping synchronization of horizontal components.

5 STRUCTURAL ANALYSIS AND FAILURE RATES

The failure rates (λ_f) shown in the following, were evaluated via equation (1):

$$\lambda_f = \int_0^{x_{10^{-5}}} P[failure | Sa(T) = x] \cdot \left| d\lambda_{Sa(T)}(x) \right| + 10^{-5}. \quad (1)$$

In the equation, $d\lambda_{Sa(T)}(x)$ is the derivative of the hazard curve of interests, and $P[\text{failure}|Sa(T)=x]$ is the failure probability of the structure for which the failure rate is being evaluated; i.e., the structural fragility. The integral stops at the last IM value ($x_{10^{-5}}$) for which hazard is computed; i.e., that with 10^{-5} annual exceedance rate. Thus, to account for this truncation 10^{-5} is added to the integral. This is an approximation that assumes structural failure, with certainty, for IMs larger than $x_{10^{-5}}$.

It has been briefly recounted in the previous section how $\lambda_{Sa(T)}$ (i.e., the seismic hazard) has been computed. For what concerns $P[\text{failure}|Sa(T)=x]$, it has been evaluated for each structure via MSA (see [3]). In particular, each (three-dimensional) structural model has been subjected to 20 records (two horizontal pairs), ad-hoc selected (see section 4) for each of ten IM values corresponding to the return periods at which probabilistic seismic hazard was computed. The sample of 20 response values collected in this way forms a so-called *stripe*, because, in a hypothetical plot of response vs IM, they are all aligned. For each stripe, the fragility was computed via equation (2):

$$P[\text{failure}|Sa(T)=x_i] = \left\{ 1 - \Phi \left[\frac{\log(edp_f) - \mu_{\log(EDP)|Sa(T)=x_i}}{\sigma_{\log(EDP)|Sa(T)=x_i}} \right] \right\} \left(1 - \frac{N_{col,Sa(T)=x_i}}{N_{tot,Sa(T)=x_i}} \right) + \frac{N_{col,Sa(T)=x_i}}{N_{tot,Sa(T)=x_i}} \quad (2)$$

where EDP is the *engineering demand parameter*, representing a structural response measure (e.g., maximum inter-storey drift ratio) and edp_f is the structural capacity for the performance of interest. The quantities $\left\{ \mu_{\log(EDP)|Sa(T)=x_i}, \sigma_{\log(EDP)|Sa(T)=x_i} \right\}$ are the mean and standard deviation of the logarithms of EDP when $Sa(T)=x_i$, $i = \{1, \dots, 10\}$, while $\Phi(\bullet)$ is the cumulative Gaussian distribution function and $N_{col,Sa(T)=x_i}$ is the number of collapse cases (i.e., those reaching global instability according to the terminology in [31]). Finally, $N_{tot,Sa(T)=x_i}$ is the number of ground-motion records, here 20, with $Sa(T)=x_i$, $i = \{1, \dots, 10\}$.

Although equation (2) is the general framework, in selected cases $P[\text{failure}|Sa(T)=x]$ has been empirically evaluated by counting the number of records for which failure has been observed, $N_{f,Sa(T)=x_i}$, as shown in equation (3).

$$P[\text{failure}|Sa(T)=x_i] = \frac{N_{f,Sa(T)=x_i}}{N_{tot,Sa(T)=x_i}} \quad (3)$$

5.1 Preliminary results

Figure 7 provides the preliminary failure rates for the buildings analyzed in 2018. The figure contemplates both the UPD as well as the GC rates for soil C. Data are arranged per increasing design hazard of the sites according to the current code. It can be seen that the trend observed in [1][3] for current-code-conforming structures, which implied decreasing reliability for increasing design hazard, is less clear for existing buildings, likely due to the large heterogeneity of the buildings analyzed. Moreover, as expected these rates are generally larger than those of new constructions. Nevertheless, these are very preliminary and are far to be

considered consolidated yet. For example, rates for UPD and GC for BI structures, needs further deepening.⁴

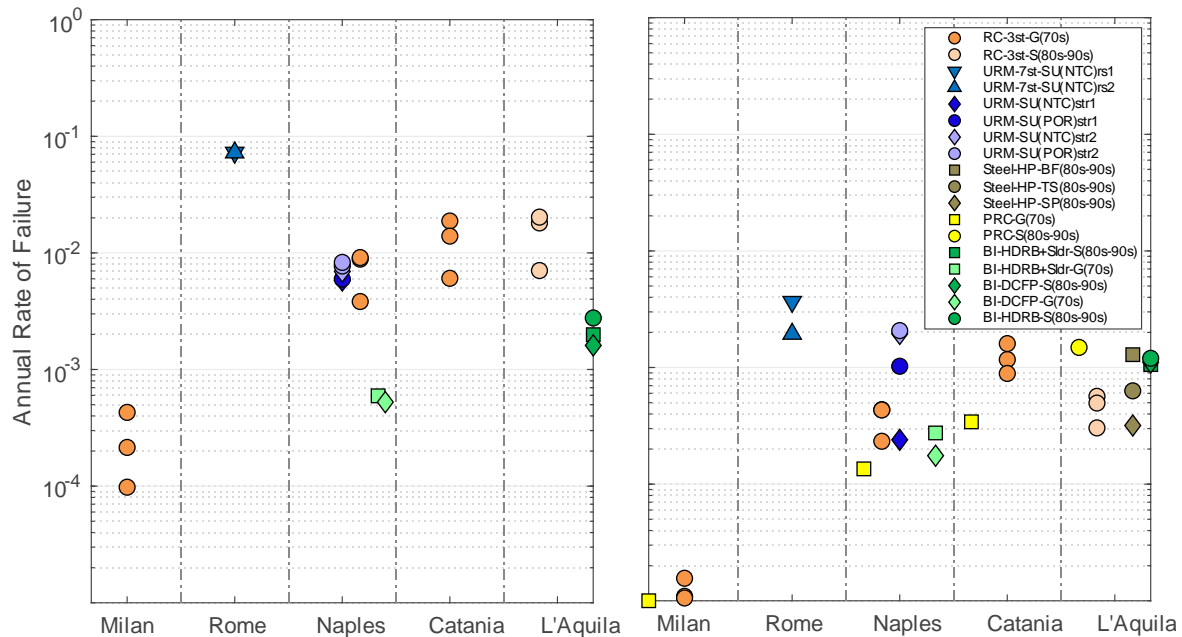


Figure 7: preliminary failure rates from the 2018 RINTC-e project for soil C; left is UPD, right is GC.

6 FINAL REMARKS

In this paper the 2019-2021 RINTC project was introduced. The project deals with the seismic reliability assessment of the existing building designed for earthquake resistance via obsolete codes or for gravity loads only. The project has the ambition to consider a wide range of Italian codes, following the evolution of construction practice in the XX century. As a preliminary work, some cases were investigated in 2018, in the framework of the RINTC-e project propaedeutic to the 2019-2021. These are mostly buildings designed according to 70s or 80s-90s codes as well as older buildings seismically upgraded according to codes from 80s-90s. Finally, base-isolated buildings are existing buildings of the mentioned type seismically upgraded according to the current code. Failure rates computed for these cases show a less clear trend with respect to what observed for current-code-conforming structures and generally higher values, as expected. Nevertheless, these results are not yet consolidated and will be likely revisited during the course of the 2019-2021 RINTC project.

7 ACKNOWLEDGEMENTS

The study was developed between 2017 and 2018 in the framework the ReLUIIS-DPC and EUCENTRE-DPC projects, funded by the *Presidenza del Consiglio dei Ministri, Dipartimento della Protezione Civile* (DPC).

8 REFERENCES

- [1] RINTC Workgroup, *Results of the 2015-2016 RINTC project*. ReLUIIS report, ReLUIIS, Naples, Italy, 2017. Available at <https://goo.gl/j8H7MV>

⁴ With regard to BI, also note that the UPD rates presented herein also include the failure of the isolation system, differently from what discussed in [13], where damage conditions were only referred to the super-structure.

- [2] I. Iervolino, A. Spillatura, and P. Bazzurro, Assessing the (Implicit) Seismic Risk of Code-Conforming Structures in Italy, in *COMPADYN 2017 - 6th ECCOMAS Thematic Conference on Computational Methods in Structural Dynamics and Earthquake Engineering*, Rhodes Island, Greece, 2017.
- [3] I. Iervolino, A. Spillatura, P. Bazzurro, Seismic reliability of code-conforming Italian buildings. *J. Earthq. Eng.*, **22**(S2), 5-27, 2018.
- [4] T. Lin, C.B. Haselton, J.W. Baker, Conditional spectrum-based ground motion selection. Part I: Hazard consistency for risk-based assessments. *Earthq. Eng. Struct. D.*, **42**, 1847-1865, 2013.
- [5] I. Iervolino, F. Petruzzelli, NODE v.1.0 beta: attempting to prioritize large-scale seismic risk of engineering structures on the basis of nominal deficit, in *XIV Convegno Nazionale L'Ingegneria Sismica in Italia*, Bari, 2011.
- [6] CS.LL.PP., Norme tecniche per le costruzioni. *Gazzetta Ufficiale della Repubblica Italiana*, **29**, 2008. (In Italian.)
- [7] CS.LL.PP., Aggiornamento delle norme tecniche per le costruzioni. *Gazzetta Ufficiale della Repubblica Italiana*, **42**, 2018. (In Italian.)
- [8] M. Stucchi, C. Meletti, V. Montaldo, H. Crowley, G.M. Calvi, E. Boschi, Seismic hazard assessment (2003–2009) for the Italian building code. *B. Seismol. Soc. Am.*, **101**, 1885-1911, 2011.
- [9] P. Ricci, V. Manfredi, F. Noto, M. Terrenzi, M.T. De Risi, M. Di Domenico, G. Camata, P. Franchin, A. Masi, F. Mollaioli, E. Spacone, G.M. Verderame, RINTC-e: Towards seismic risk assessment of existing residential reinforced concrete buildings in Italy, in *COMPADYN 2019 - 7th ECCOMAS Thematic Conference on Computational Methods in Structural Dynamics and Earthquake Engineering*, Crete, Greece, 2019.
- [10] G. Magliulo, D. Bellotti, C. Di Salvatore, F. Cavalieri, RINTC-e project: towards the seismic risk of low and pre-code single-story r/c precast buildings in Italy, in *COMPADYN 2019 - 7th ECCOMAS Thematic Conference on Computational Methods in Structural Dynamics and Earthquake Engineering*, Crete, Greece, 2019.
- [11] S. Bracchi, S. Cattari, S. Degli Abbatì, S. Lagomarsino, G. Magenes, M. Mandirola, S. Marino, A. Penna, M. Rota, RINTC-e project: towards the seismic risk of retrofitted existing Italian URM buildings, in *COMPADYN 2019 - 7th ECCOMAS Thematic Conference on Computational Methods in Structural Dynamics and Earthquake Engineering*, Crete, Greece, 2019.
- [12] G. Cantisani, G. Della Corte, RINTC-e: Seismic risk of pre-code single-story non-residential steel buildings in Italy, in *COMPADYN 2019 - 7th ECCOMAS Thematic Conference on Computational Methods in Structural Dynamics and Earthquake Engineering*, Crete, Greece, 2019.
- [13] L. Ragni, D. Cardone, N. Conte, A. Dall'Asta, A. Di Cesare, A. Flora, N. Lamarucciola, F. Micozzi, F. Ponzio, RINTC-e project: the seismic risk of existing Italian RC buildings retrofitted with seismic isolation, in *COMPADYN 2019 - 7th ECCOMAS Thematic Conference on Computational Methods in Structural Dynamics and Earthquake Engineering*, Crete, Greece, 2019.
- [14] MIN.LL.PP., Decreto ministeriale 2 luglio 1981. *Gazzetta Ufficiale della Repubblica Italiana*, **198**, 1981. (In Italian.)

- [15] MIN.LL.PP., Circolare 30 luglio 1981, Istruzioni relative alla normativa tecnica per la riparazione ed il rafforzamento degli edifici in muratura danneggiati dal sisma, Rome, Italy. (In Italian.)
- [16] M. Tomažević, *The computer program POR*, Report ZRMK, Institute for Testing and Research in Materials and Structures, Ljubljana, Slovenia, 1978. (In Slovenian.)
- [17] CS.LL.PP., Norme tecniche per la esecuzione delle opere in cemento armato normale e precompresso e per le strutture metalliche. *Gazzetta Ufficiale della Repubblica Italiana*, **198**, 1974. (In Italian.)
- [18] CS.LL.PP., Norme tecniche per le opere in c.a. normale e precompresso e per le strutture metalliche. *Gazzetta Ufficiale della Repubblica Italiana*, **65**, 1992. (In Italian.)
- [19] CS.LL.PP., Norme tecniche relative alle costruzioni antisismiche. *Gazzetta Ufficiale della Repubblica Italiana*, **108**, 1986. (In Italian.)
- [20] C.N.R., *UNI 10012-67 – Ipotesi di carico sulle costruzioni*. UNI, Milan, Italy, 1967. (in Italian.)
- [21] CS.LL.PP., Istruzioni relative ai carichi, ai sovraccarichi ed ai criteri generali per la verifica di sicurezza delle costruzioni. *Gazzetta Ufficiale della Repubblica Italiana*, **140**, 1982.
- [22] C.N.R., *UNI 10011-88 – Costruzioni di acciaio: istruzioni per il calcolo, l'esecuzione, il collaudo e la manutenzione*. UNI, Milan, Italy, 1988. (in Italian.)
- [23] C.E.N., Eurocode 8: *Design of Structures for Earthquake Resistance: Part 1: General Rules, Seismic Actions and Rules for Buildings*, European Committee for Standardization, Bruxelles, Belgium, 2004.
- [24] S. Barani, D. Spallarossa, P. Bazzurro, Disaggregation of probabilistic ground-motion hazard in Italy. *B. Seismol. Soc. Am.*, **99**, 2638-2661, 2009.
- [25] N.N. Ambraseys, K.U. Simpson, J.J. Bommer, Prediction of horizontal response spectra in Europe. *Earthq. Eng. Struct. D.*, **25**, 371-400, 1996.
- [26] S. Akkar, J.J. Bommer, Empirical Equations for the Prediction of PGA, PGV, and Spectral Accelerations in Europe, the Mediterranean Region, and the Middle East. *Seismol. Res. Lett.*, **81**, 195-206, 2010.
- [27] D. Monelli, M. Pagani, G. Weatherill, V. Silva, H. Crowley, The hazard component of OpenQuake: The calculation engine of the Global Earthquake Model, in *15WCEE - 15th world conference on earthquake engineering*, Lisbon, Portugal, 2012.
- [28] L. Luzi, S. Hailemikael, D. Bindi, F. Pacor, F. Mele, F. Sabetta, ITACA (ITalian AC-celerometric Archive): a web portal for the dissemination of Italian strong-motion data, *Seismol. Res. Lett.*, **79**, 716-722, 2008.
- [29] T.D. Ancheta, R.B. Darragh, J.P. Stewart, et al., NGA-West2 database. *Earthq. Spectra*, **30**, 989-1005, 2014.
- [30] R. Dobry, I.M. Idriss, E. Ng, Duration characteristics of horizontal components of strongmotion earthquake records. *B. Seismol. Soc. Am.*, **68**, 1487-1520, 1978.
- [31] N. Shome, C.A. Cornell, Structural seismic demand analysis: Consideration of "Collapse", in *PMC2000 - 8th ASCE Specialty Conference on Probabilistic Mechanics and Structural Reliability*. University of Notre Dame, South Bend, Indiana, 2000.